J. Appl. Comput. Mech., 7(2) (2021) 798-810
DOI: 10.22055/JACM.2020.35529.2676

ISSN: 2383-4536
jacm.scu.ac.ir

Shahid Chamran University of Ahvaz

Journal of Applied and Computational Mechanics

Research Paper

Sensitivity Analyses of Structural Damage Indicators and Experimental Validations

Jiqiao Zhang[1], Zhiqiang Teng[2], Xiaojian Xu[3], Gongfa Chen[4], David Bassir[5]

[1] School of Civil and Transportation Engineering, Guangdong University of Technology, Guangzhou, 510006, China, Email: zhangjq@gdut.edu.cn

[2] School of Civil and Transportation Engineering, Guangdong University of Technology, Guangzhou, 510006, China, Email: tzq1217@sina.cn

[3] School of Civil and Transportation Engineering, Guangdong University of Technology, Guangzhou, 510006, China, Email: xuxj@gdecn.com

[4] School of Civil and Transportation Engineering, Guangdong University of Technology, Guangzhou, 510006, China, Email: gongfa.chen@gdut.edu.cn

[5] Centre Borelli, CMLA, ENS Cachan, CNRS, Université Paris-Saclay, 94235 Cachan, France, Email: david.bassir@utbm.fr

Received October 26 2020; Revised December 23 2020; Accepted for publication December 23 2020.
Corresponding author: G. Chen (gongfa.chen@gdut.edu.cn)

Abstract. The vibration-based damage detection (VBDD) has been widely used in structural health monitoring (SHM). However, different damage indicators have different effects on SHM. It is necessary to analyze the sensitivity of structural damage indicators to study the correlation between these indicators and damages. In this paper, the sensitivities of the mode shape, modal strain energy (MSE) and strain mode are numerically studied and experimentally validated. The damage is simulated by the reduction in the cross-sectional area of the rods of a 3-D steel frame. The sensitivity of the three damage indicators are obtained and compared by using the finite element (FE) analyses of the frame; the modal parameters are obtained through the experimental modal analysis, and the sensitivity of the three damage indicators are calculated to validate whether they could identify the structural damage. The results indicate that, generally, the sensitivity of the modal strain is the highest, followed by the MSE, and the sensitivity of the mode shape is the lowest. Nevertheless, the MSE shows high sensitivity in the cases of multiple damages. The sensitivity of the damage indicators varies for different damage locations; the sensitivity decreases from the mid span to the end of the steel frame. The above results provide a theoretical basis for the selection of damage indicators in the damage detection.

Keywords: Structural Damage Detection, Sensitivity Analysis, Damage Indicator, Experimental Modal Analysis, Finite Element Analysis

1. Introduction

Early detection and repair of structural damages in civil engineering is of great significance to ensure the safety and service life of structures and prevent catastrophic events [1]. The traditional structural damages detection (SDD) method, visual inspection by experienced engineers, is subjective, time-consuming and laborious. Because of their flexibility, cost-effectiveness and non-destructiveness, the vibration-based damage detection (VBDD) methods have become a research hotspot in SHM [2, 3]. The basic idea of VBDD technology is that the changes in the physical properties (stiffness, mass and damping) of a structure will lead to changes in its modal parameters (frequency, mode shape and strain energy), which are functions of its physical properties [4]. Hence, the changes in the modal parameters can be assumed as indictors for damage detection. At present, a few damage detection indicators have been developed , including: natural frequency , flexibility matrix, mode shape , strain mode and modal strain energy [5-7]. Kim et al. [8] proposed a single damage indicator method to locate and quantify a crack in beam-type structures by using changes in a few natural frequencies. A crack location model and a crack size model are established to identify the damage by cleverly linking the modal energy fraction change with the damage induced natural frequency change. The rotating-spring crack modeling based on fracture mechanics will lose credibility in the case of hig h frequency mode or deep cracks. Therefore, these methods are only applicable to long and thin beam structures with s mall cracks. Compared with the natural frequencies, the advantages of using mode shapes and their derivatives as the basic features of damage detection are obvious [10]. Modal shapes contain local information, which makes them more sensitive to local damage and less sensitive to environmental effects (such as temperature) than their natural frequencies. Hu et al. [11] pr oposed a statistical algorithm for damage detection based on the difference of modal shapes of wooden beams before a nd after damage. The effectiveness of the algorithm was verified by numerical simulations of different damage degrees, damage locations and damage combinations. The damage indicators derived from the mode shapes also have ideal damage detection effect. Among them, the mode shape curvature and the MSE were widely used in SHM [12]. Frans et al. [13] overcame the shortcoming of low order modal shapes by applying modal curvature to the damage identification of three types of structures. Ding et al. [14] proposed a damage index based the MSE method for girder road and bridge structures. Numerically

Published online: December 24 2020

applying the method to a bridge using a continuous beam model resulted in a good agreement with assumed damages at different locations with various quantities. Compared with the detection methods derived from the displacement modal parameters, the research on the strain-based damage detection methods started relatively late. As small structural defects can be more easily detected through the change of strain rather than the change of displacement, the strain-related detection methods have attracted more and more attention recently [15-18]. Swamidas and Chen [19] carried out modal analysis of cantilever plates with small cracks based on finite element method. It was found that most of the modal parameters, such as natural frequency, response amplitude and mode shape, were affected by surface cracks, and modal strain identification was the best among the tested methods. In recent years, post-processing technology for damage indicators had been developed gradually (e.g., principle component analysis [20], wavelet transform [21, 22], bat optimization [23-25], and Machine Learning [2 6] [27]). Zhong et al. [26] combined the modal shape with the convolutional neural network to effectively identify the damage location of the bar. Whether the selected damage indicator can contain more damage characteristics will affect the final results of structural damages detection [28], while the effectiveness of a damage detection indicator is determined by its sensitivity to structural damages.

Structural sensitivity is widely used in structural optimization, FE model modification and structural damage detection [29-31]. The sensitivity analysis methods commonly used in engineering include the derivative method, finite difference method and perturbation method. In the sensitivity analysis, the sensitivity of any eigenvector (i.e., mode shape) was expressed as a linear combination of all eigenvectors [32]. However, this method needed to know all the modal information. Subsequently, a new algorithm of the eigenvector sensitivity was proposed, which only needs the first order modal information [33]. Then, a new algebraic algorithm was proposed, which can simultaneously calculate the sensitivity of a eigenvalue and eigenvector; it is also computationally efficient [34, 35]. As an actual structure always has damp, so many scholars have studied the eigen-sensitivity of a damped system. Sensitivity calculation begins to consider the influence of modified mass in viscous damped systems and extends to nonlinear damped systems [36, 37]. The sensitivity analysis is mostly based on the matrix theory of discrete systems, and the matrix calculation conceals the influence of damage parameters on the sensitivity of damage indicators. At present, there are few comparisons between the sensitivity of various damage detection methods based on a continuum model [38].

Most of the above mentioned methods used a modal parameter as damage index to detect structural damage without comparing its sensitivity, which represents its ability to reflect the changes of structural features caused by structural damage. In this paper, a variety of damage scenarios were set to explore the sensitivity of different damage detection indicators in a nu merical 3-D steel frame. To introduce a damage indictor for structural damage detection, one essential issue is to effectively evaluate its sensitivity to the variation of structural parameters. The sensitivity of modal parameters is derived by using the model method [39], from which, the MSE sensitivity is obtained by using an indirect method (The indirect method is based on the existing sensitivity method of mode shape) [40]; and the modal strain sensitivity is obtained through the strain modal analysis. The FE model of the steel frame is established. The modal parameters of damaged and intact cases are extracted by FE analysis, and the sensitivity of three damage indicators are calculated according to the derived formula. The sensitivity of the three indicators to damage were compared and validated by vibration experiments.

2. Theory

The vibration of a multiple-degree-of-freedom system can be described by the following equation:

$$\mathbf{M}\ddot{\mathbf{x}} + \mathbf{C}\dot{\mathbf{x}} + \mathbf{K}\mathbf{x} = \mathbf{0} \tag{1}$$

where, $\mathbf{M}$, $\mathbf{C}$ and $\mathbf{K}$ are the mass, damping and stiffness matrices of the system, respectively. From Eq. (1), we can get:

$$\mathbf{K}\Phi_i = \omega_i^2 \mathbf{M}\Phi_i \tag{2}$$

where ω_i and Φ_i are the i-th modal frequency and mode shape.

The sensitivity of a mode shape can be expressed as its derivative against a variable p, which can be expanded as a linear combination of all eigenvectors [40]:

$$\frac{d\Phi_i}{dp} = \sum_{k=1}^{N} c_k \Phi_k \tag{3}$$

with

$$c_k = \begin{cases} \dfrac{\Phi_k^T}{\omega_k^2 - \omega_i^2}\left(-\dfrac{d\mathbf{K}}{dp} + \omega_i^2 \dfrac{d\mathbf{M}}{dp}\right)\Phi_i & k \neq i \\ -\dfrac{1}{2}\Phi_k^T \dfrac{d\mathbf{M}}{dp}\Phi_k & k = i \end{cases} \tag{4}$$

As the mass matrix $\mathbf{M}$ is non-singular, the eigenvectors are usually normalized as

$$\Phi_i^T \mathbf{M}\Phi_i = 1 \tag{5}$$

for the i-th eigenvector, the global MSE can be expressed as

$$\mathrm{MSE}_i = \frac{1}{2}\Phi_i^T \mathbf{K}\Phi_i \tag{6}$$

for the j-th element, the MSE can be then expressed by

$$\mathrm{MSE}_{ji} = \frac{1}{2}\Phi_i^T \mathbf{K}_j \Phi_i \tag{7}$$

where $\mathbf{K}_j$ is the elemental stiffness matrix. Therefore, the sensitivity of the modal strain energy can be expressed as:

$$\frac{d\mathrm{MSE}_{ji}}{dp} = \Phi_i^T \mathbf{K}_j \frac{d\Phi_i}{dp} + \frac{1}{2}\Phi_i^T \frac{d\mathbf{K}_i}{dp}\Phi_i \tag{8}$$

According to the FE theory, the relationship between the strain mode shape $\boldsymbol{\psi}_i^{\varepsilon}$ and displacement mode shape Φ is:

$$\boldsymbol{\psi}_i^{\varepsilon} = \mathbf{C}\Phi_i \tag{9}$$

with

$$\mathbf{C} = \mathbf{BT}\boldsymbol{\delta} \tag{10}$$

where $\mathbf{B}$ is the strain matrix, $\mathbf{T}$ is the coordinate transformation matrix between the elemental coordinate system and global coordinate system, $\boldsymbol{\delta}$ is nodal displacement vector. Here

$$\mathbf{B} = \frac{1}{l^2}\left[-6+\frac{12x}{l} \quad -4l+6 \quad 6-\frac{12x}{l} \quad -2l-6x\right], \mathbf{T} = \begin{bmatrix} \cos\theta & 0 & 0 & 0 \\ 0 & 1 & & \\ 0 & & \cos\theta & \\ 0 & & & 1 \end{bmatrix}, \text{ and } \boldsymbol{\delta} = \left\{v_i \quad w_i \quad v_j \quad w_j\right\}^T.$$

Substituted Eq. (9) into Eq. (2), we can get:

$$\left(\mathbf{K} - \omega_i^2 \mathbf{M}\right)\mathbf{C}^{-1}\boldsymbol{\psi}_i^{\varepsilon} = 0 \tag{11}$$

therefore, the sensitivity of strain mode can be expressed as:

$$\frac{d\boldsymbol{\psi}_i^{\varepsilon}}{dp} = \frac{1}{m}\sum_{i=1}^{m}\frac{\Delta\Psi_i^{\varepsilon}}{\Psi_i^{\varepsilon}} \tag{12}$$

where m is the number of the effective mode shapes.

3. Numerical Simulations

3.1 Model

This paper used a steel frame as the structural model (Fig. 1a). The steel frame had the length, width and height of 10.61 m, 0.354 m and 0.354 m respectively, and consists of 381 rods; each rod had a hollow circular cross section with the external radius of 0.005 m and thickness of 0.002 m. The software package, ABAQUS (SIMULIA Inc, Providence, RI, USA), was used to build a FE model of the steel frame used in the vibration experiments (Fig. 1b). The density, elastic modulus, Poisson's ratio and modal damping were 7800 kg/m^3 , 212 GPa , 0.28 and 0.02, respectively. The model was meshed with beam element and restricted at the two ends of the steel structure. It was assumed that the structural damage was proportional to the reduction of the elastic modulus, i.e., the damage of 50% was simulated by reducing the elastic modulus of the rod to its half.

3.2 Comparison of the sensitivity of three damage detection indicators

Rod 56 (as shown in Fig. 2) was replaced with a damaged rod; the FE input file was modified and submitted for analysis. Finally, the sensitivities of the 3 indicators at all the 381 rods in the model were obtained in ABAQUS post-processing, and the obtained sensitivity of each damage indicator was normalized against its maximum value. The results were shown in Fig. 3.

Figure 3 showed that the sensitivity of the strain mode was highest and that of the mode shape was lowest; also the strain mode had the best anti-interference ability to the surrounding elements, while the mode shape fails to indicate the damage location at all.

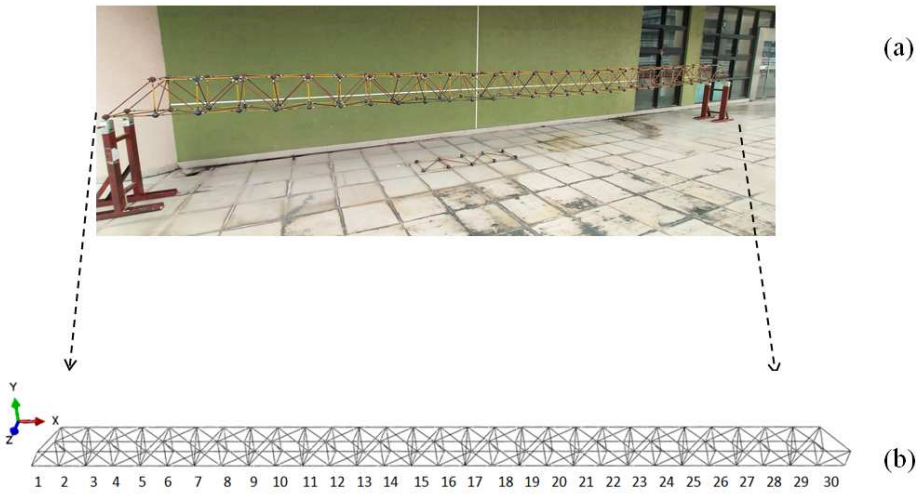

Fig. 1. Steel frame with 381 rods. (a) Experimental model, (b) FE model.

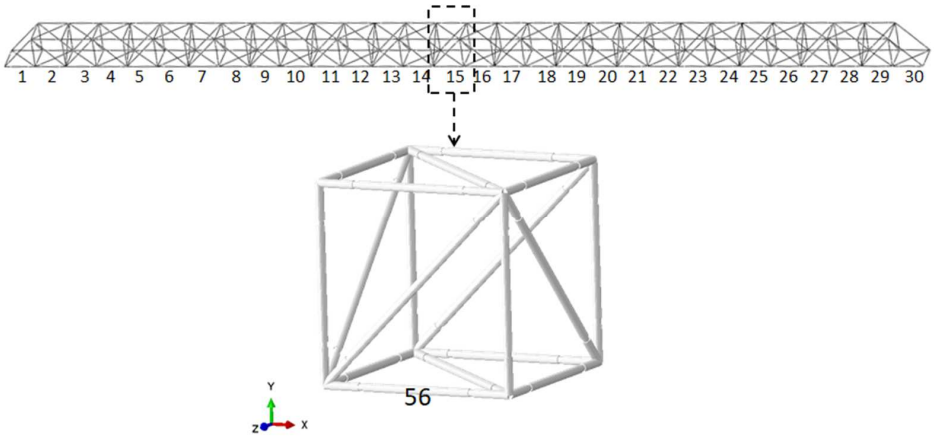

Fig. 2. Location of Rod 56.

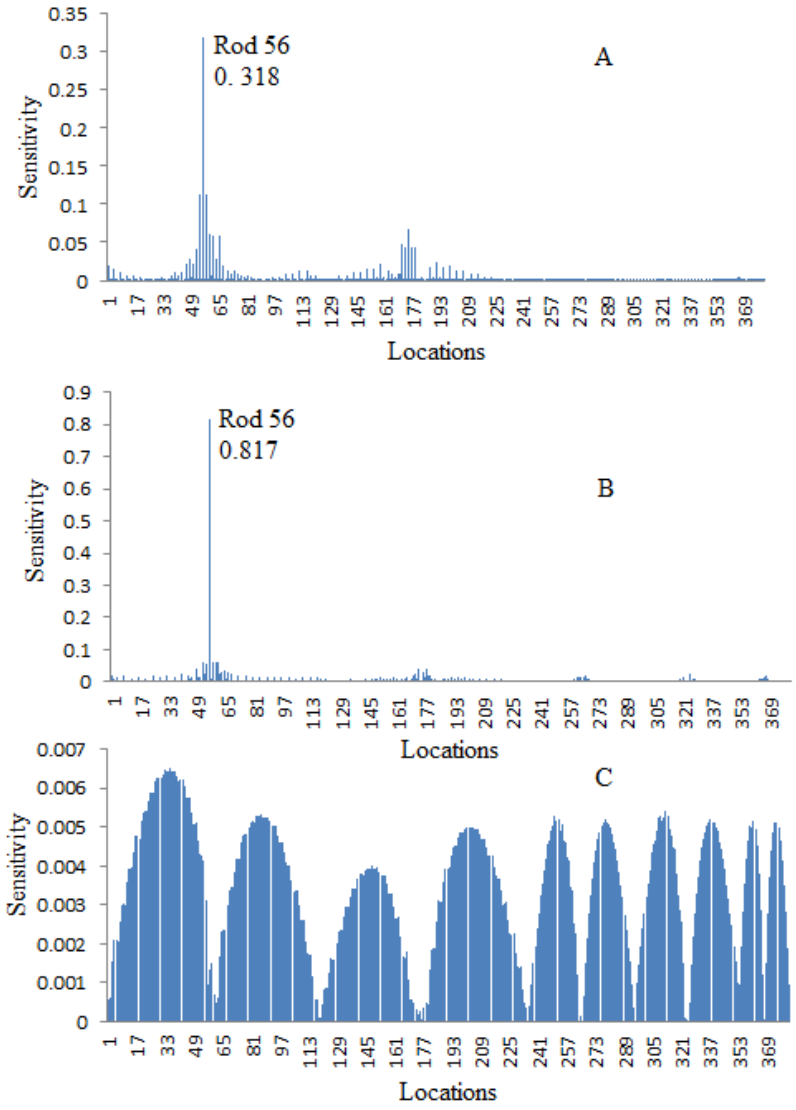

Fig. 3. Sensitivities of three damages indicators to damage of Rod 56: (A) modal strain energy; (B) strain mode; (C) mode shapes.

3.3 The relationship between damage indicator sensitivity and damage location

In order to find the relationship between the sensitivity of the damage indicators and the damage location, 10 scenarios were designed, which included the 50% damage in Rods 60, 62, 72, 74, 84, 86, 96, 98, 108 and 110 (Fig. 4) respectively. The normalized sensitivity in the horizontal and vertical directions could be obtained by comparing the 10 scenarios. The distributions of the normalized sensitivity of the damage indicators against the 10 damaged rods were shown in Fig. 5.

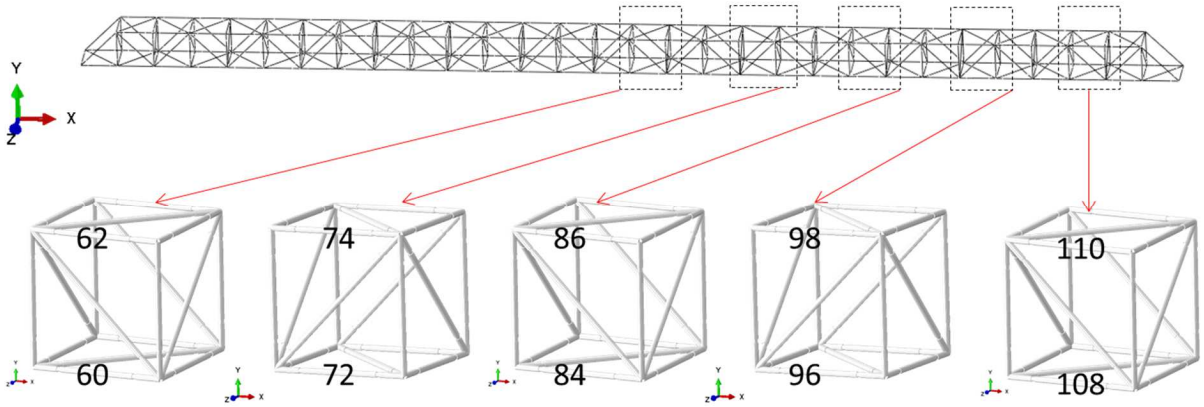

Fig. 4. Location distribution of the damaged rod.

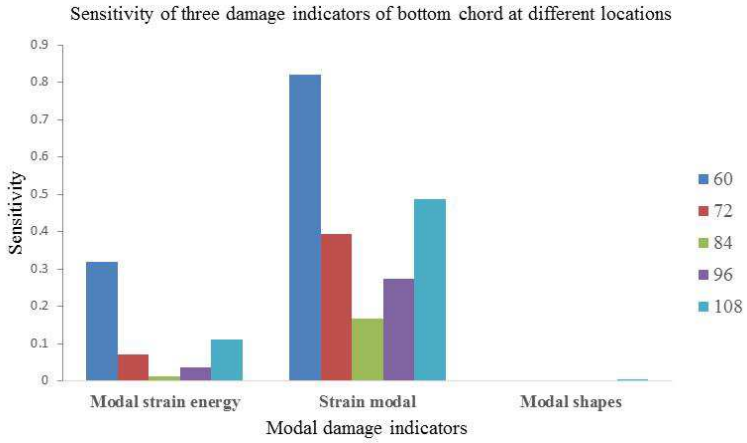

(a) Sensitivity of damage indicators of bottom chord

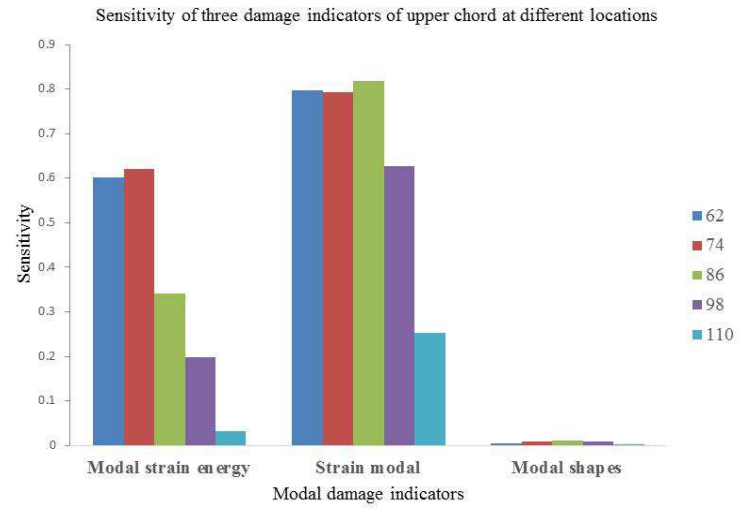

(b) Sensitivity of damage indicators of upper chord

Fig. 5. Sensitivity of damage indicators for different damage locations in horizontal direction.

The results (Fig. 5) show that the sensitivity of damage indicators decreases from mid spans to end spans, that is, the damage indicator was more sensitive to the damage in mid spans.

3.4 The sensitivity of damage indicators for different rods damaged

In order to find out the sensitivity variation of the three damage indicators for different types of rods, 9 kinds of damage scenarios were designed with one damage rod for each scenario; the damage rod was Rod 59, Rod 60, Rod 61, Rod 62, Rod 265, Rod 266, Rod 324, Rod 325 and Rod 367, respectively. Among them, Rod 60 and Rod 62 were parallel to the X-axis, Rod 59 was parallel to the Y-axis, Rod 265 and Rod 324 were parallel to the Z-axis, Rod 61 was a diagonal parallel to the X-Y plane, Rod 266 and Rod 325 were diagonals parallel to the X-Z plane, and Rod 367 was a diagonal parallel to the Y-Z plane (Fig. 6). The distributions of the normalized sensitivity were shown in Fig. 7.

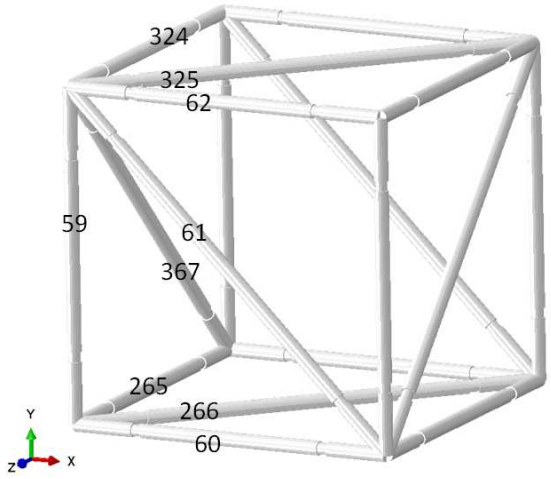

Fig. 6. Damage locations of steel frame structures of different damage states scenarios.

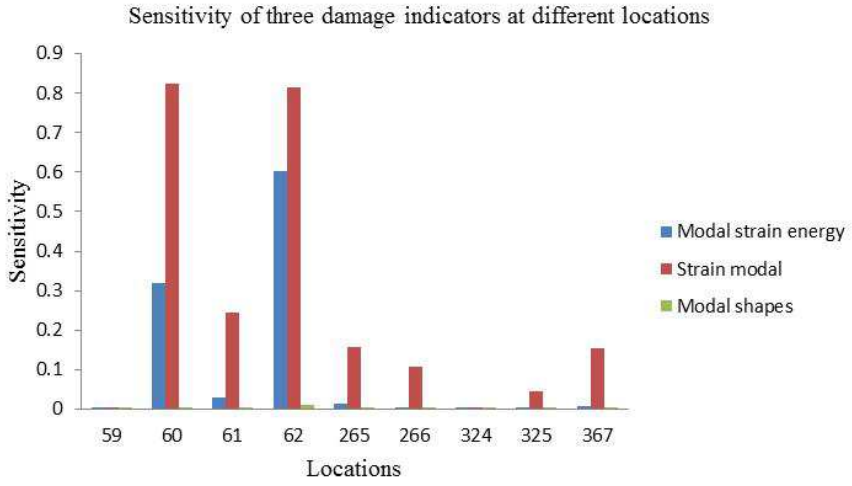

Fig. 7. Sensitivity for different damage indicators of the steel frame.

Figure 7 showed that, the sensitivity of the damage indicators was highest at the Rod 60 and Rod 62 and was almost zero at the Rod 59 and Rod 324, while it was relatively low at the other rods. The above results show that: the sensitivity of the damage indicators was high in the members parallel to the X-axis (Rod 60 and Rod 62), while it was low in the members parallel to the Y-axis and Z-axis (Rod 59 and Rod 324); the sensitivity was between the above two scenarios in diagonal web members (Rods 61, 325, and 367).

4. Experimental Validation

4.1 Experimental model and equipment

Figure 1a showed the steel frame used in the experiments. Experimental equipment (Fig. 8) included a dynamic data acquisition instrument (JM3840, Jing-Ming Technology Inc., Yangzhou, China), intact and damaged rods, accelerometers, strain gauges, a hammer and a laptop. Modal analyses were carried out with JM3840 software. The experimental modal analysis can be found in He and Fu [41].

4.2 Experimental setup and procedure

In this experiment, 17 rods within four spans in the middle were selected for the study, and the rods and acceleration measurement points were numbered (55-71 were the number of the rods and · -· were the location of the acceleration measurement points in Fig. 9). The damage was introduced in Rod 56 and Rod 65 by cutting off 50% of its cross-sectional area, the damage scenarios were shown in Table 1. The structural damage detection process is shown in Fig. 10.

Table 1. Experimental damage scenarios

Datasets	Damage scenarios	Damaged locations	Damage level (%)
1	No damage	—	—
2	Single damage	56	50%
3	Single damage	65	50%
4	Double damage	56, 65	50%, 50%

Fig. 8. Experimental devices. (a) Acquisition instrument, (b) Laptop, (c) Intact and damaged rods, (d) Strain gage, (e) Impact hammer, (f) Accelerometers.

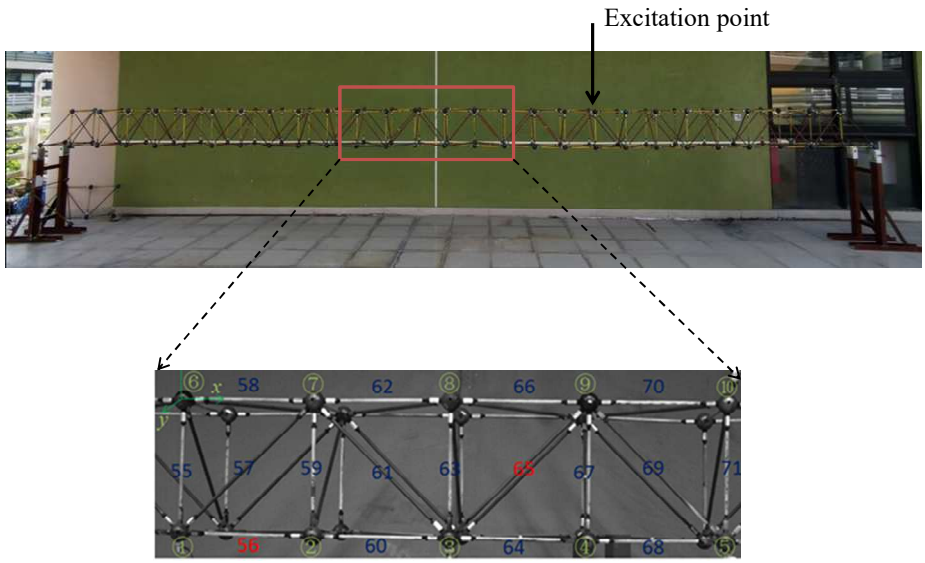

Fig. 9. Measurement points and rods numbering.

This experiment adopts the method of single-point excitation and multi-point acquisition. For accelerometer measurement: (1) In the area of interest shown in Fig. 11, the acceleration sensors were arranged on 10 bolt balls respectively (Fig. 11a). As the steel frame weighs 135 kg, while the accelerometers weigh 0.50 kg and the cable 0.84 kg, therefore, the effect of the added mass (of the accelerometers and cable) on the measurement results can be ignored. (2) The frequency response function of each measurement point was analyzed by the modal analysis software. (3) The natural frequency and mode shape of the vibration system were extracted from the frequency response function. (4) The obtained vertical mode data were used to calculate the modal strain energy difference and mode shape difference of the elements. For strain gauge measurement: (1) the strain gauges were arranged on Rods 55-71 (Fig. 11b); (2) the strain frequency response function of each measurement point was analyzed by the modal analysis software; (3) the natural frequency and strain mode of the vibration system were extracted from the strain frequency response function; (4) the obtained strain mode was used to calculate the strain mode difference.

4.3 Experimental data

Figure 12 was the time-history curve of the excitation force and the corresponding time-history curves of acceleration (measured 1 to 10 nodes) are showed Figure 13. Figure 14 showed the time-history curves of strain. The sampling frequency was 250 Hz and the sampling time was 20.5 s.

4.4 The modal identification

The modal parameters of the structure were obtained by the modal analysis of the collected excitation (force), acceleration and strain signals.. Tables 2 and 3were the mode shape of different structural states, and the calculation of rotation was based on the formula presented in [42].

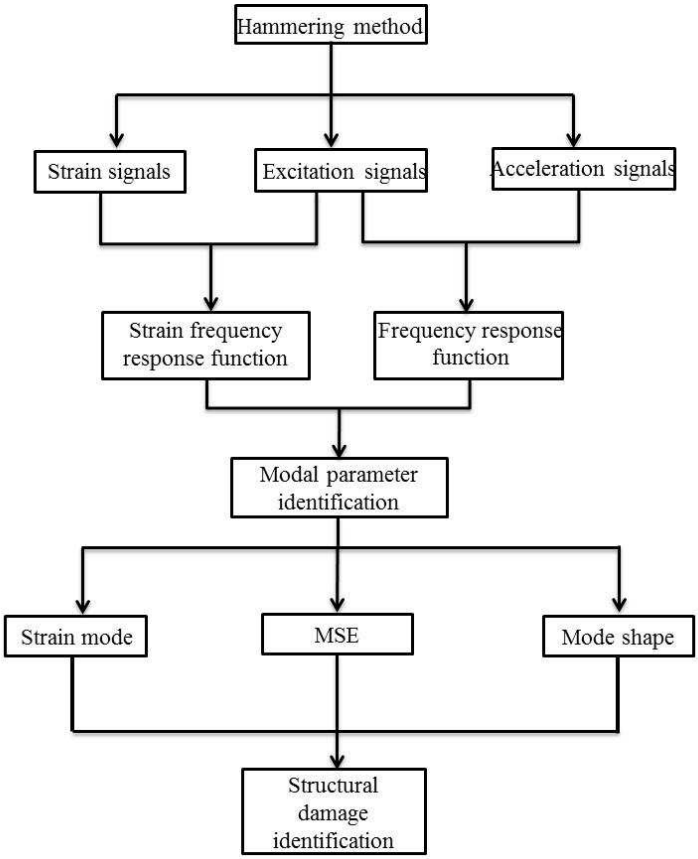

Fig. 10. Structural damage detection process.

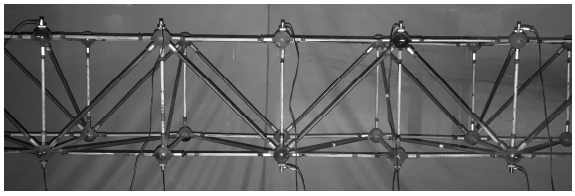

(a) Accelerometer

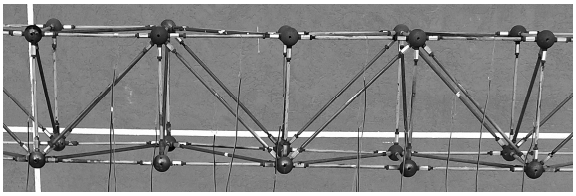

(b) Strain gauge

Fig. 11. Arrangement of acceleration sensors and strain gauges.

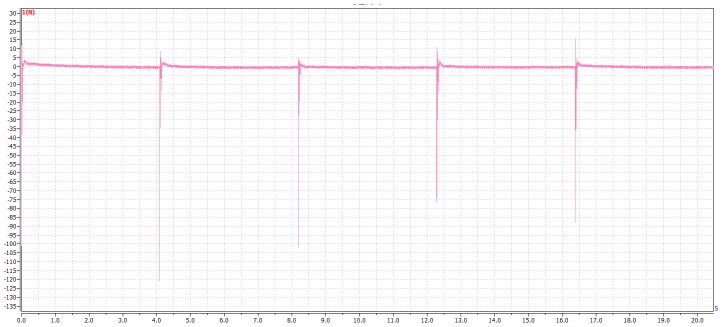

Fig. 12. The time-history curve of force.

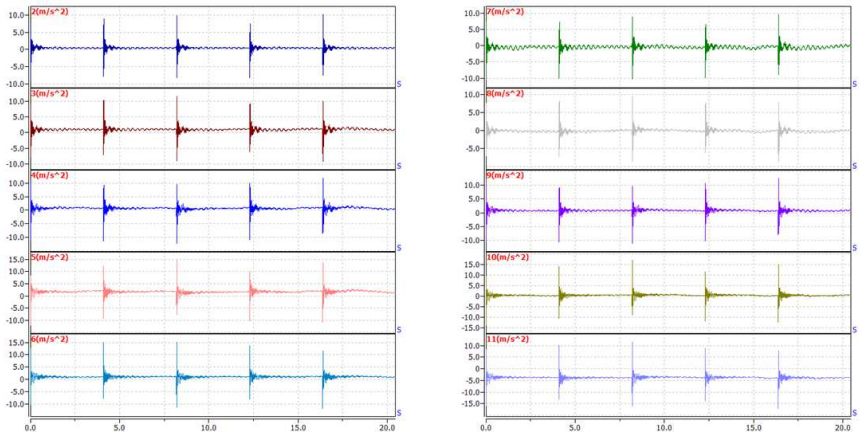

Fig. 13. Time history curves of acceleration at each measurement point.

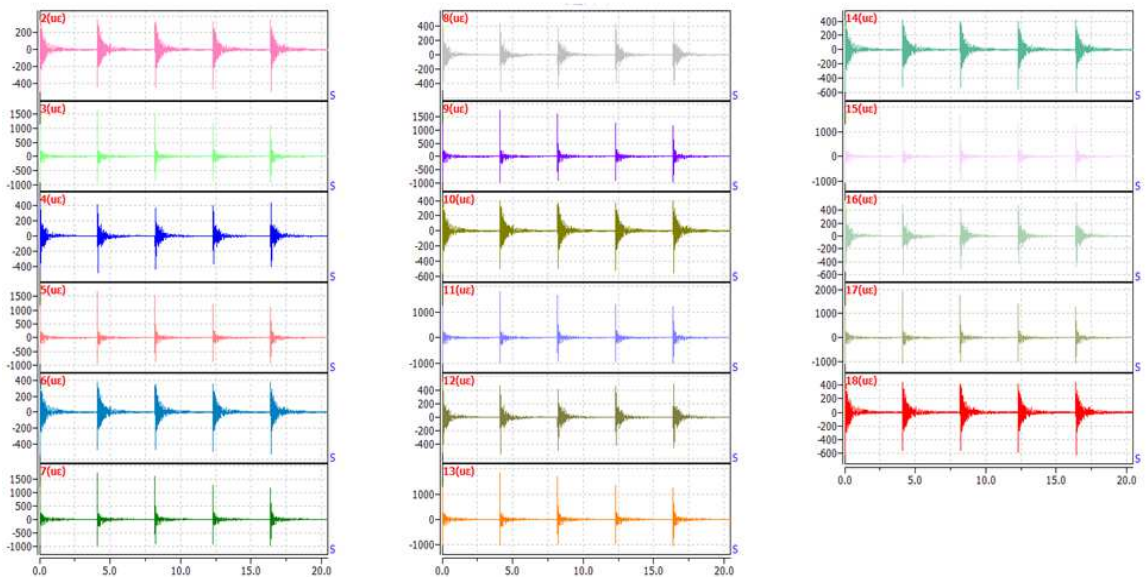

Fig. 14. The time-history curves of the strain.

Table 2. The first-order mode shape based on acceleration

Rods	Scenario (1)	Scenario(2)	Scenario (3)	Scenario (4)
	Mode shape	Mode shape	Mode shape	Mode shape
1	0.645	0.058	0.655	0.275
2	0.641	0.105	0.627	0.401
3	0.624	0.080	0.625	0.298
4	0.551	0.055	0.606	0.234
5	0.535	0.043	0.537	0.241
6	0.615	0.193	0.599	0.570
7	0.665	0.105	0.651	0.357
8	0.646	0.089	0.649	0.309
9	0.606	0.081	0.524	0.180
10	0.558	0.062	0.544	0.261

Table 3. The first-order mode shape based on strain

Rods	Scenario (1)	Scenario(2)	Scenario (3)	Scenario (4)
	Strain mode	Strain mode	Strain mode	Strain mode
55	0.019	0.097	0.050	0.015
56	0.025	0.922	0.090	0.724
57	0.151	0.069	0.015	0.058
58	0.524	0.427	0.572	0.329
59	0.305	0.181	0.434	0.140
60	0.099	0.214	0.065	0.020
61	0.073	0.012	0.016	0.037
62	0.514	0.533	0.529	0.484
63	0.200	0.099	0.054	0.142
64	0.681	0.736	0.532	0.765
65	0.120	0.139	0.617	0.656
66	0.484	0.521	0.425	0.430
67	0.013	0.030	0.016	0.004
68	1.000	1.000	1.045	0.891
69	0.014	0.038	0.008	0.014
70	0.057	0.040	0.153	0.040
71	0.054	0.124	0.022	0.028

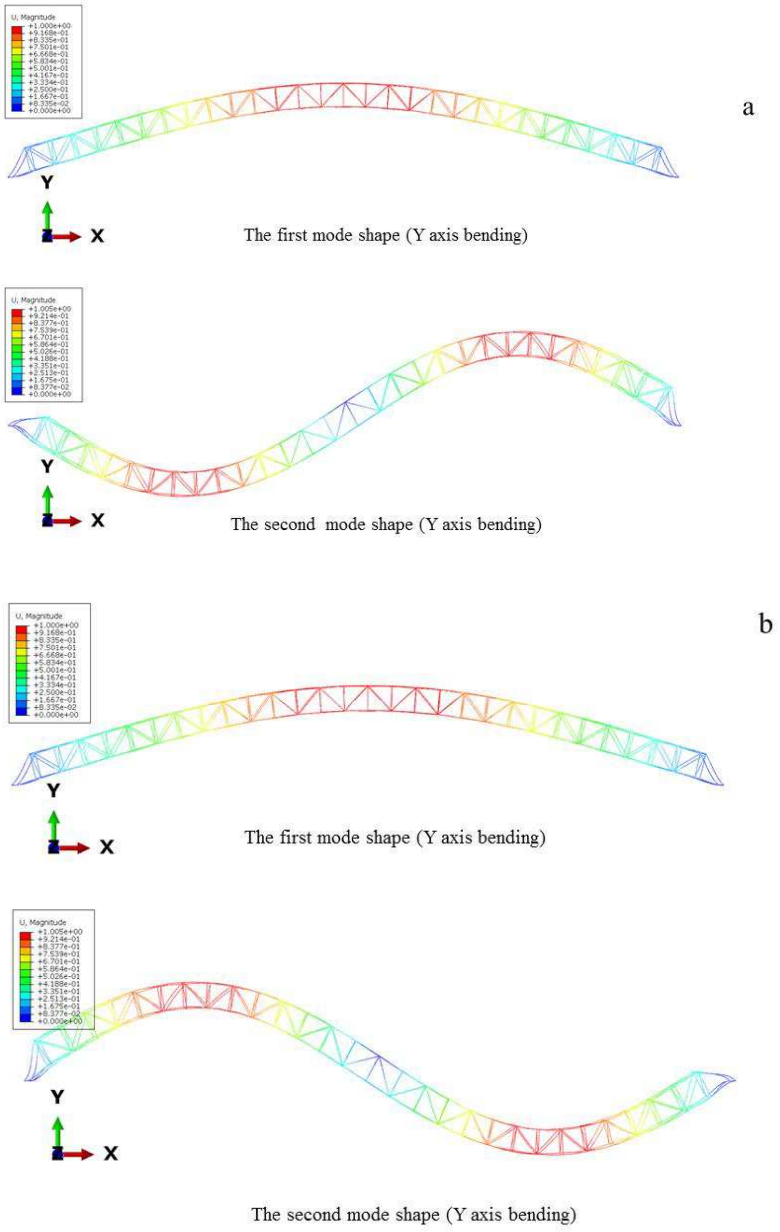

Fig. 15. (a) The first two mode shapes of undamaged scenario, (b) The first two mode shapes of damage scenario.

By using the FEM, the mode shapes of the structures before and after damage can be obtained, as shown in Table 2 (Take the first two modes).

The results show that the structural damage has little effect on the mode shapes, and the change of mode shapes cannot be used as damage indicators to evaluate the damage scenario of the 3-D steel frame.

Table 4. MSE difference under different damage scenario based on acceleration

Rods	Scenario (2)	Scenario (3)	Scenario (4)
55	0.000000	0.000005	0.000001
56	1.000000	0.129700	1.000000
57	0.003420	0.011411	0.002919
58	0.818418	0.261580	0.785717
59	0.000022	0.000115	0.000025
60	0.199271	0.307902	0.184819
61	0.011932	0.013281	0.012153
62	0.594592	0.978202	0.539161
63	0.000004	0.000185	0.000009
64	0.128280	0.035422	0.126151
65	0.001976	0.249049	0.011611
66	0.594453	1.000000	0.538249
67	0.000018	0.000314	0.000028
68	0.093777	0.256131	0.099496
69	0.006104	0.015123	0.006406
70	0.387141	0.512262	0.386317
71	0.000007	0.000015	0.000006

Table 5. The modal strain difference based on strain

Rods	Scenario (2)	Scenario (3)	Scenario (4)
55	0.000377	0.000213	0.000364
56	1.000000	0.049357	1.000000
57	0.010054	0.012646	0.008867
58	0.122602	0.075217	0.113771
59	0.004201	0.002903	0.003985
60	0.079570	0.066252	0.072919
61	0.029486	0.001790	0.029128
62	0.088521	0.133134	0.075219
63	0.000054	0.022194	0.001651
64	0.055394	0.026904	0.052369
65	0.010254	1.000000	0.468042
66	0.084746	0.148929	0.070252
67	0.000305	0.002830	0.000511
68	0.039121	0.015134	0.039235
69	0.008010	0.008768	0.008507
70	0.056396	0.014920	0.052823
71	0.000225	0.000116	0.000204

Table 6. The mode shape differences based on acceleration

Rods	Scenario (2)	Scenario (3)	Scenario (4)
55	0.751284	0.133017	1.000000
56	0.037417	0.116390	0.095018
57	0.239912	0.121140	0.352399
58	0.327219	0.125891	0.463100
59	0.091709	0.147268	0.055351
60	0.091709	0.308789	0.240775
61	0.052091	0.306413	0.190037
62	0.086574	0.216152	0.200185
63	0.381511	0.194774	0.561808
64	0.553925	0.304038	0.572878
65	0.562729	1.000000	0.313653
66	0.559795	0.166271	0.630996
67	0.740279	0.771971	0.598708
68	0.854732	0.781473	0.738007
69	0.878210	0.755344	0.778598
70	0.877476	0.755344	0.778598
71	1.000000	0.679335	0.965867

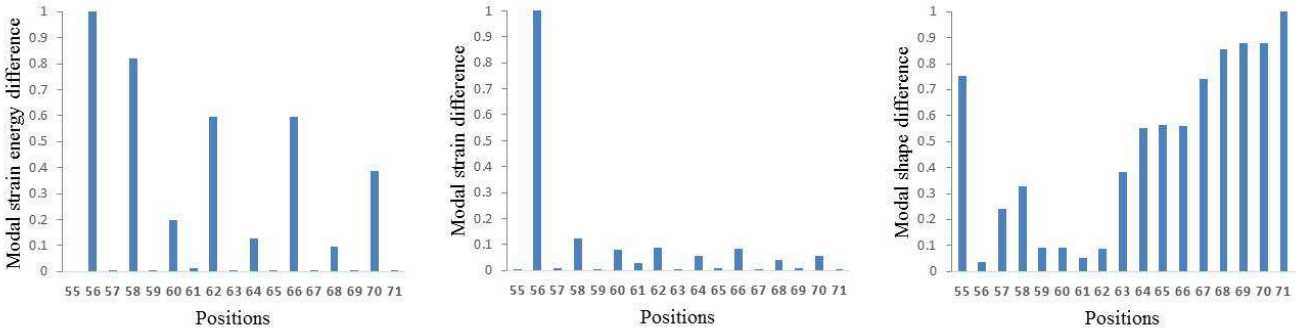

Fig. 16. Sensitivity of the three damage indicators for Scenario 2.

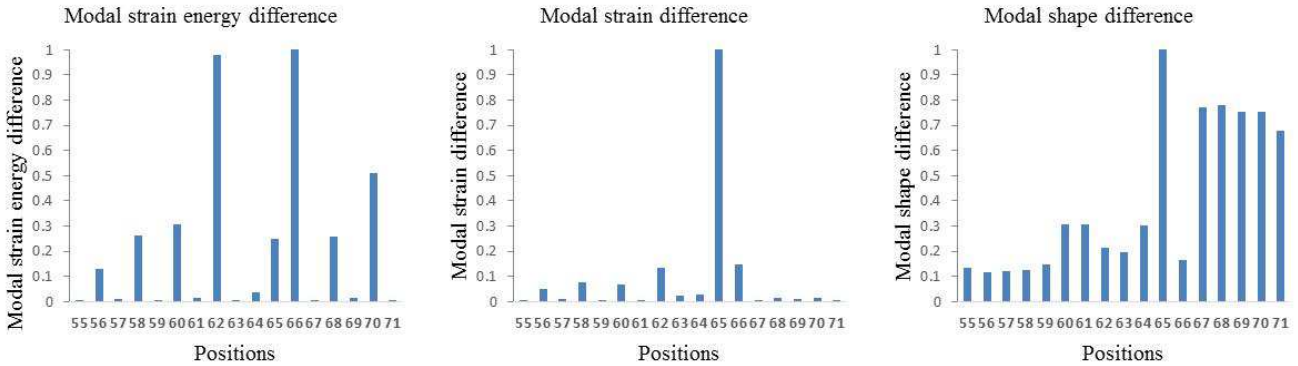

Fig. 17. Sensitivity of the three damage indicators for Scenario 3.

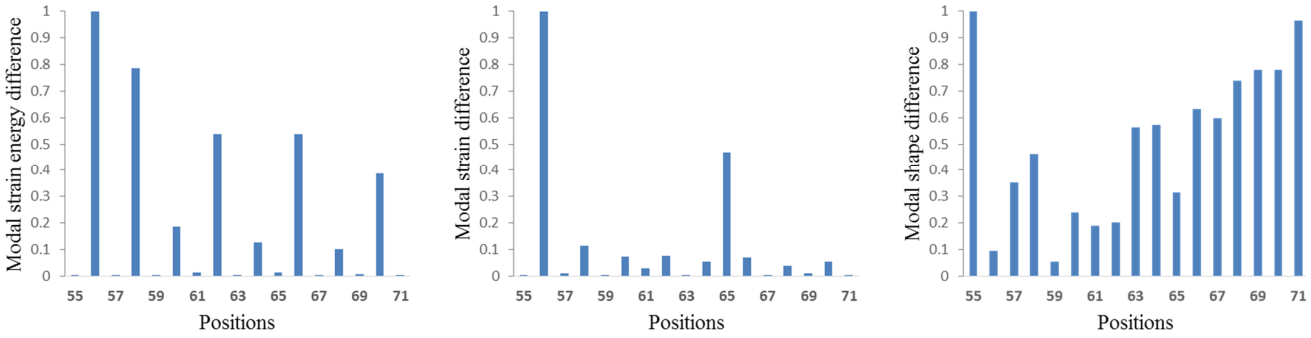

Fig. 18. Sensitivity of the three damage indicators for Scenario 4.

4.5 Damage localization results and comparison

From the first-order mode shape in Table 2, the MSE of each element was calculated by using Formula (7). In order to compare their variation with damage location, each of the three damage detection indicators was normalized against its maximum value, as shown in Table 4 to 6.

Figures 16-18 show the sensitivity variations of the three damage indicators under different damage scenarios listed in Table 4 to 6.

Figure 16 showed that both MSE difference and strain mode difference can identify the damage location in Scenario 2. However, compared with the MSE difference, the identification effect of strain mode difference is better. The mode shape performed even worse without identifying the damaged rod. Figure 17 showed that in Scenario 3, the strain mode difference still had a high sensitivity in detection of Rod 65 (diagonal web member). Compared with the identification of No. 56 rod, the mode shape difference is better for the identification of No. 65 rod; however, the MSE has a poor performance in the identification of inclined ventral rods. However, the modal strain energy was not good for the detection of diagonal web members.

Figure 18 showed that the identifications of multiple damages, the strain mode indicator still showed evident detection, while the modal strain energy and mode shape were not good enough in detecting the damage location, and they were easily disturbed by the surrounding members.

From the above results, it could be seen that the damage identification effect of the three damage indicators were different whether in the same damage scenarios or different damage scenarios. The identification effect of a certain damage indicator was good in one scenario, but was not good enough in other scenarios.

5. Conclusions

The numerical simulation results in Section 3 showed that the sensitivities of the three damage indicators perform differently; the sensitivity of the damage indicators in the steel frame showed certain patterns. The experimental results in Section 4 validated the sensitivity of the three damage detection indicators obtained in Section 3 (the higher the sensitivity of the damage indicator, the better the damage identification effect). It was found that the sensitivity of three detection indicators in the steel frame was affected by damage location and rod types; in the case of multiple damages, the damage rods will affect each other. In the process of damage detection, we can combine the global method with the local method. First, we can use the VBDD indicators to roughly judge the damage existence, and then make a detailed examination to confirm the damage part in the local area, which is helpful to avoid the problem of insufficient sensitiveness of the damage detection indicators under some working conditions.

Based on the above discussion, the following conclusions can be drawn:

1. Under the same condition, the sensitivity of the three damage detection indicators ranges from high to low as follows: strain mode, MSE, and mode shape.
2. The sensitivity of the damage detection indicator in the steel frame varies with damage location.
3. The sensitivity of damage indicators to the damage of different members (in-plane and out of plane) in the same span is different.
4. For the damage indicators which are more sensitive to structural damage, its sensitivity is more prominent in a variety of damage conditions or more complex damage conditions.

Author Contributions

J. Zhang and G. Chen planned the scheme, initiated the project, and suggested the experiments; Z. Teng and X. Xu conducted the experiments and analyzed the empirical results; D. Bassir developed the mathematical modeling and examined the theory validation. The manuscript was written through the contribution of all authors. All authors discussed the results, reviewed, and approved the final version of the manuscript.

Conflict of Interest

The authors declared no potential conflicts of interest with respect to the research, authorship, and publication of this article.

Funding

The support from Program of Study Abroad for Young Scholar in Guang Dong University of Technology is acknowledged.

References

[1] Zimoch Z. Sensitivity analysis of vibrating systems. *Journal of Sound & Vibration*, 1987, 115(3): 447-58.
[2] Chang, K.C., Kim, et al. Modal-parameter identification and vibration-based damage detection of a damaged steel truss bridge. *Engineering Structures*, 2016, 122: 156-173.
[3] Farahani R.V., Penumadu D. Damage identification of a full-scale five-girder bridge using time-series analysis of vibration data. *Engineering Structures*, 2016, 115: 129-39.
[4] Yan Y.J., Cheng L., Wu Z.Y., et al. Development in Vibration-Based Structural Damage Detection Technique. *Mechanical Systems & Signal Processing*, 2007, 21(5): 2198-211.
[5] Li B., Li Z., Zhou J., et al. Damage localization in composite lattice truss core sandwich structures based on vibration characteristics. *Composite Structures*, 2015, 126: 34–51.
[6] Dawari V.B., Kamble P.P., Vesmawala G.R. Structural Damage Identification Using Modal Strain Energy Method. *Advances in Structural Engineering*, 2015, 2599-607.
[7] Shi Z.Y., Law S.S., Zhang L.M. Structural Damage Detection from Modal Strain Energy Change. *American Society of Civil Engineers*, 2014, 126(12): 1216-23.
[8] Kim J.T., Stubbs N. Crack detection in beam-type structures using frequency data. *Journal of Sound & Vibration*, 2003, 259(1): 145-60.
[9] Döhler M., Hille F., Mevel L., et al. Structural health monitoring with statistical methods during progressive damage test of S101 Bridge. *Engineering Structures*, 2014, 69(9): 183-93.
[10] Dutta A., Talukdar S. Damage detection in bridges using accurate modal parameters. *Finite Elements in Analysis & Design*, 2004, 40(3): 287-304.
[11] Hu C., Afzal M.T. A statistical algorithm for comparing mode shapes of vibration testing before and after damage in timbers. *Journal of Wood Science*, 2006, 52(4): 348-52.
[12] Wu S., Zhou J., Rui S., et al. Reformulation of elemental modal strain energy method based on strain modes for structural damage detection. *Advances in Structural Engineering*, 2016, 20(6): 896-905.
[13] Frans R., Arfiadi Y., Parung H. Comparative study of mode shapes curvature and damage locating vector methods for damage detection of structures. *Procedia Engineering*, 2017, 171: 1263-71.
[14] Ding Q., Zou C., Tang Y., et al. *Damage Detection in Roads and Bridges Based on Modal Strain Energy Method*. Proceedings of the International Conference on Transportation Engineering, 2013: 1753-1758.
[15] Kahl K., Sirkis J.S. Damage detection in beam structures using subspace rotation algorithm with strain data. *AIAA Journal*, 2015, 34(12): 2609-14.
[16] Abdel Wahab M.M., De Roeck G. Damage Detection in Bridges Using Modal Curvatures: Application to a Real Damage Scenario. *Journal of Sound & Vibration*, 1999, 226(2): 217-35.
[17] Liang Y.C., Hwu C. On-line identification of holes/cracks in composite structures. *Smart Materials & Structures*, 2001, 10(4): 599.
[18] Ndambi J.M., Vantomme J., Harri K. Damage assessment in reinforced concrete beams using eigenfrequencies and mode shape derivatives. *Engineering Structures*, 2002, 24(4): 501-15.
[19] Swamidas A.S.J., Chen Y. Monitoring crack growth through change of modal parameters. *Journal of Sound and Vibration*, 1995, 186(2): 325-43.
[20] Dackermann U., Smith W.A., Randall R.B. Damage identification based on response-only measurements using cepstrum analysis and artificial neural networks. *Structural Health Monitoring*, 2014, 13(4): 430-444.
[21] Liu Y.Y., Ju Y.F., Duan C.D., et al. Structure damage diagnosis using neural network and feature fusion. *Engineering Applications of Artificial Intelligence*, 2011, 24(1): 87-92.
[22] Li Z., Park H.S., Adeli H. New method for modal identification of super high-rise building structures using discretized synchrosqueezed wavelet and Hilbert transforms. *The Structural Design of Tall and Special Buildings*, 2017, 26(3): 1-16.
[23] Gomes G.F., Chaves J.A.S., Almeida F.A.D. An inverse damage location problem applied to AS-350 rotor blades using bat optimization algorithm and multiaxial vibration data. *Mechanical Systems and Signal Processing*, 2020, 145: 106932.
[24] Gomes G.F., Pereira J.V.P. Sensor placement optimization and damage identification in a fuselage structure using inverse modal problem and firefly algorithm. *Evolutionary Intelligence*, 2020, 13: 571–591.
[25] Ferreira G.G., Alves D.A.F., Simes D.C.S., et al. An estimate of the location of multiple delaminations on aeronautical CFRP plates using modal data inverse problem. *International Journal of Advanced Manufacturing Technology*, 2018, 99: 1155–1174.
[26] Zhong K., Teng S., Liu G., et al. Structural Damage Features Extracted by Convolutional Neural Networks from Mode Shapes. *Applied Sciences*, 2020, 10(12): 4247.
[27] Teng S., Chen G., Gong P., et al. Structural damage detection using convolutional neural networks combining strain energy and dynamic response. *Meccanica*, 2020, 55: 945–959.
[28] Doebling S.W., Farrar C.R., Prime M.B. A Summary Review of Vibration-Based Damage Identification Methods. *Shock & Vibration Digest*, 1998, 30(2): 91-105.
[29] Saltelli A., Chan K., Scott E.M. *Sensitivity Analysis*. John Wiley and Sons, New York, 2000.
[30] Aloisio A., Battista L.D., Alaggio R., et al. Sensitivity analysis of subspace-based damage indicators under changes in ambient excitation covariance, severity and location of damage. *Engineering Structures*, 2020, 208: 110235.
[31] Morassi A., Vestroni F. Dynamic methods for damage detection in structures. *Lectures of the CISM Course*, 2008.
[32] Stubbs N., Kim J.T. Damage localization in structures without baseline modal parameters. *AIAA Journal*, 2012, 34(8): 1644-9.
[33] Nelson R.B. Simplified calculation of eigenvector derivatives. *AIAA Journal*, 1976, 14(9): 1201-5.
[34] Lee I., Jung G. An efficient algebraic method for the computation of natural frequency and mode shape sensitivities—Part I. Distinct natural frequencies. *Computers & Structures*, 1997, 62(3): 429-435
[35] Lee I.-W., Jung G.-H. An efficient algebraic method for the computation of natural frequency and mode shape sensitivities—Part II. Multiple natural frequencies. *Computers & Structures*, 1997, 62(3): 437-43.
[36] Friswell M.I., Adhikari S. Derivatives of complex eigenvectors using Nelson's method. *AIAA Journal*, 2000, 38: 2355-2357.
[37] Adhikari S. Rates of Change of Eigenvalues and Eigenvectors in Damped Dynamic System. *AIAA Journal*, 1999, 37(11): 1452-8.
[38] Chen G., Gong P.P., Liang P. Sensitivity analyses of resonant frequencies and modal strain energy of damaged beams by perturbation method. *Journal of Vibroengineering*, 2019, 21(1): 40-51.
[39] Li L., Hu Y., Wang X., et al. Eigensensitivity analysis of damped systems with distinct and repeated eigenvalues. *Finite Elements in Analysis & Design*, 2013, 72: 21-34.
[40] Li L., Hu Y., Wang X. Numerical methods for evaluating the sensitivity of element modal strain energy. *Finite Elements in Analysis & Design*, 2013, 64: 13-23.
[41] He J., Fu Z.-F. *Modal analysis*. Oxford, Boston: Butterworth-Heinemann, 2001.
[42] Guan H., Karbhari V.M. Improved damage detection method based on Element Modal Strain Damage Index using sparse measurement. *Journal of Sound & Vibration*, 2008, 309(3-5): 465-94.

How to cite this article: Zhang J., Teng Z., Xu X., Chen G., Bassir D. Sensitivity Analyses of Structural Damage Indicators and Experimental Validations, *J. Appl. Comput. Mech.*, 7(2), 2021, 798–810. https://doi.org/10.22055/JACM.2020.35529.2676